25 mM and further with 42 mM glucose (n = 6). (D) Representative time course of $[ATP]_c$ and $[Ca^{2+}]_c$ in an islet stimulated with various levels of glucose. Glucose levels were increased in a stepwise manner from 2.8 to 25 mM (n = 12). The black line represents $[ATP]_c$ and the red line represents $[Ca^{2+}]_c$.

FIGURE 9. Dynamics of $[ATP]_c$ and $[Ca^{2+}]_c$ when glucose-induced $[Ca^{2+}]_c$ oscillations were stopped. (A) Representative time course of $[ATP]_c$ and $[Ca^{2+}]_c$ in islets showing $[Ca^{2+}]_c$ oscillations, treated with 4 μM CCCP (n = 5). Islets were incubated in KRH medium containing 25 mM glucose. (B) Representative time course of $[ATP]_c$ and $[Ca^{2+}]_c$ in islets upon reduction of the glucose concentration (n = 5). The black line represents $[ATP]_c$ and the red line represents $[Ca^{2+}]_c$.

FIGURE 10. Dependence of glucose-induced intracellular ATP elevation on intracellular Ca^{2+}. (A-D) The effect of Ca^{2+} depletion from the medium. $[ATP]_m$ (A, B) or $[ATP]_c$ (C, D) was monitored in isolated islets when the glucose level was elevated from 2.8 to 20 mM (n = 5 for both (A) and (C), n = 6 for both (B) and (D), respectively). Islets were pretreated with Ca^{2+}-depleted KRH medium (A, C) or normal Ca^{2+}-containing KRH medium (B, D) for 40 minutes. (E, F) The effect of intracellular Ca^{2+} depletion. $[ATP]_m$ (E) or $[ATP]_c$ (F) were monitored in isolated islets when the glucose level was elevated from 2.8 to 20 mM (n = 5 for both (E) and (F), respectively). Islets were pretreated with 5 μM 1,2-bis(o-aminophenoxy)ethane-N,N,N′,N′-tetraacetic acid (BAPTA)-AM (BAPTA) for 20 minutes. (G) Depletion of intracellular Ca^{2+} decreases basal $[ATP]_m$. Time course of $[ATP]_m$ in islets treated with 5 μM BAPTA-AM (BAPTA). Islets were incubated in KRH medium containing 2.8 mM glucose (n = 5).

Downloaded from http://www.jbc.org/ at Kyoto University on December 24, 2013

Figure 1

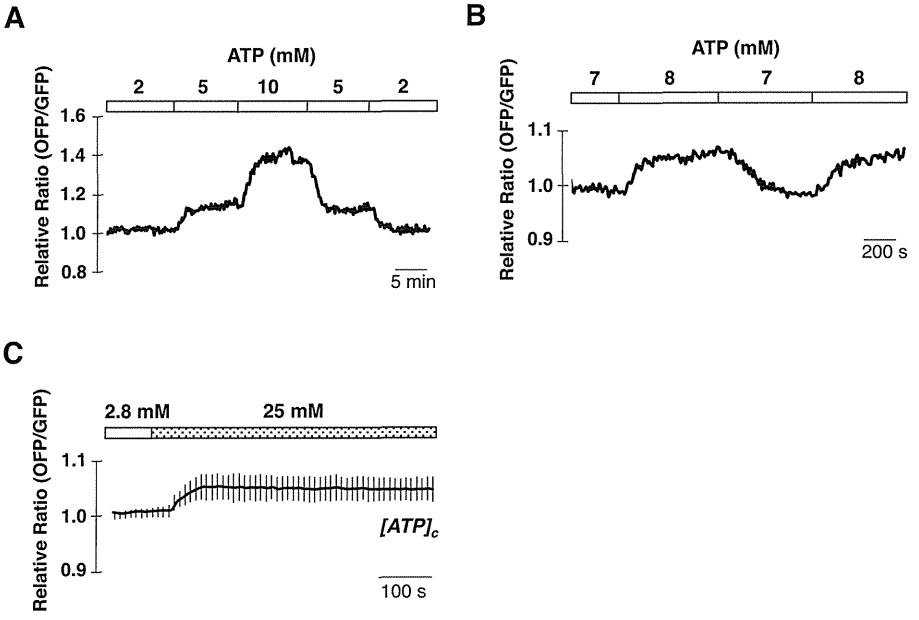

Downloaded from http://www.jbc.org/ at Kyoto University on December 24, 2013

Figure 2

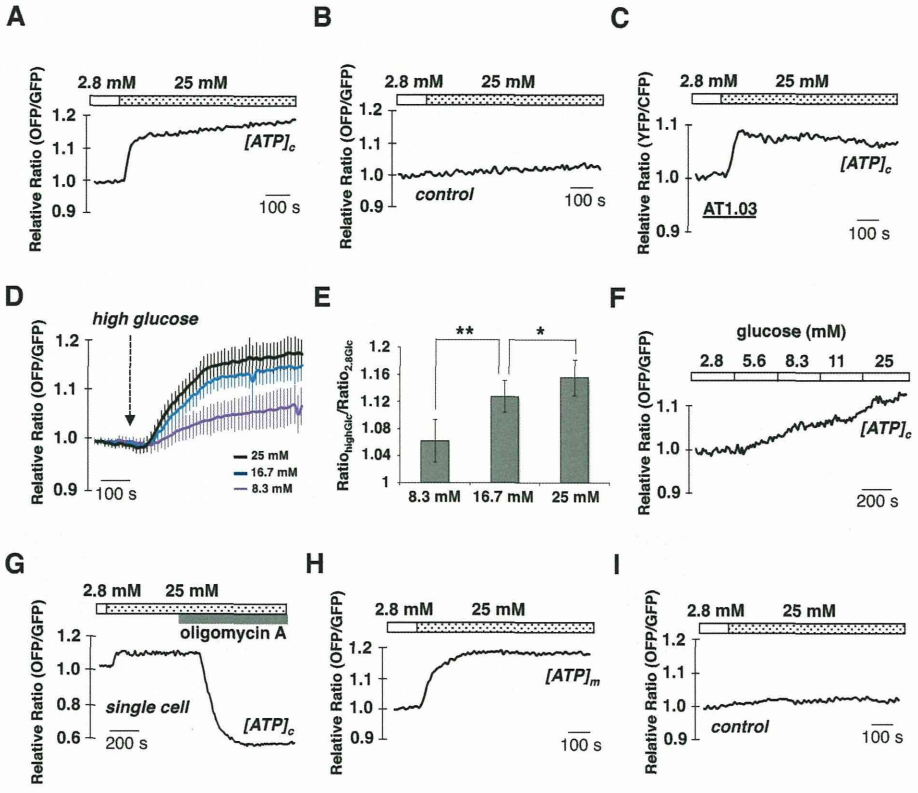
A
2.8 mM
25 mM
Relative Ratio (OFP/GFP)
[ATP]c
100 s
B
control
C
Relative Ratio (YFP/CFP)
AT1.03
D
high glucose
25 mM
16.7 mM
8.3 mM
E
Ratio$_{HighGlc}$/Ratio$_{2.8Glc}$
8.3 mM
16.7 mM
25 mM
F
glucose (mM)
2.8
5.6
8.3
11
25
200 s
G
oligomycin A
single cell
H
[ATP]m
I

Figure 3

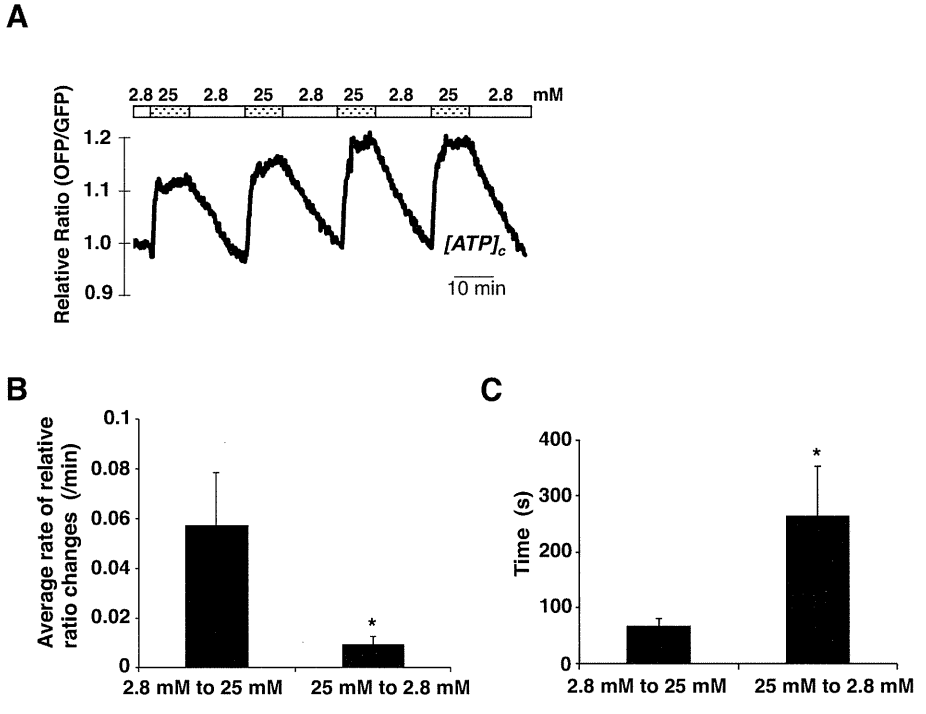
A
2.8 25 2.8 25 2.8 25 2.8 25 2.8 mM
Relative Ratio (OFP/GFP)
1.2
1.1
1.0
0.9
[ATP]c
10 min
B
Average rate of relative ratio changes (/min)
0.1
0.08
0.06
0.04
0.02
0
*
2.8 mM to 25 mM
25 mM to 2.8 mM
C
Time (s)
400
300
200
100
0
*
2.8 mM to 25 mM
25 mM to 2.8 mM

Figure 4

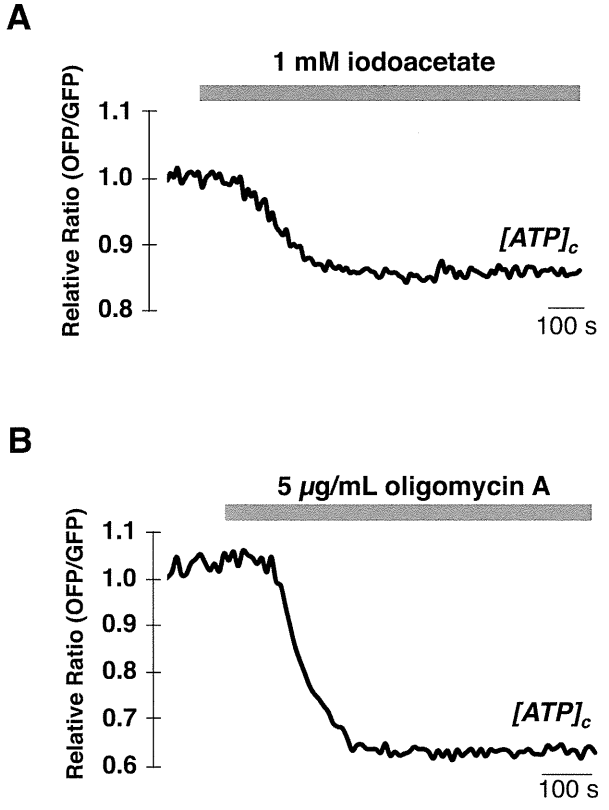
A
1 mM iodoacetate
Relative Ratio (OFP/GFP)
1.1
1.0
0.9
0.8
[ATP]c
100 s
B
5 μg/mL oligomycin A
Relative Ratio (OFP/GFP)
1.1
1.0
0.9
0.8
0.7
0.6
[ATP]c
100 s

Figure 5

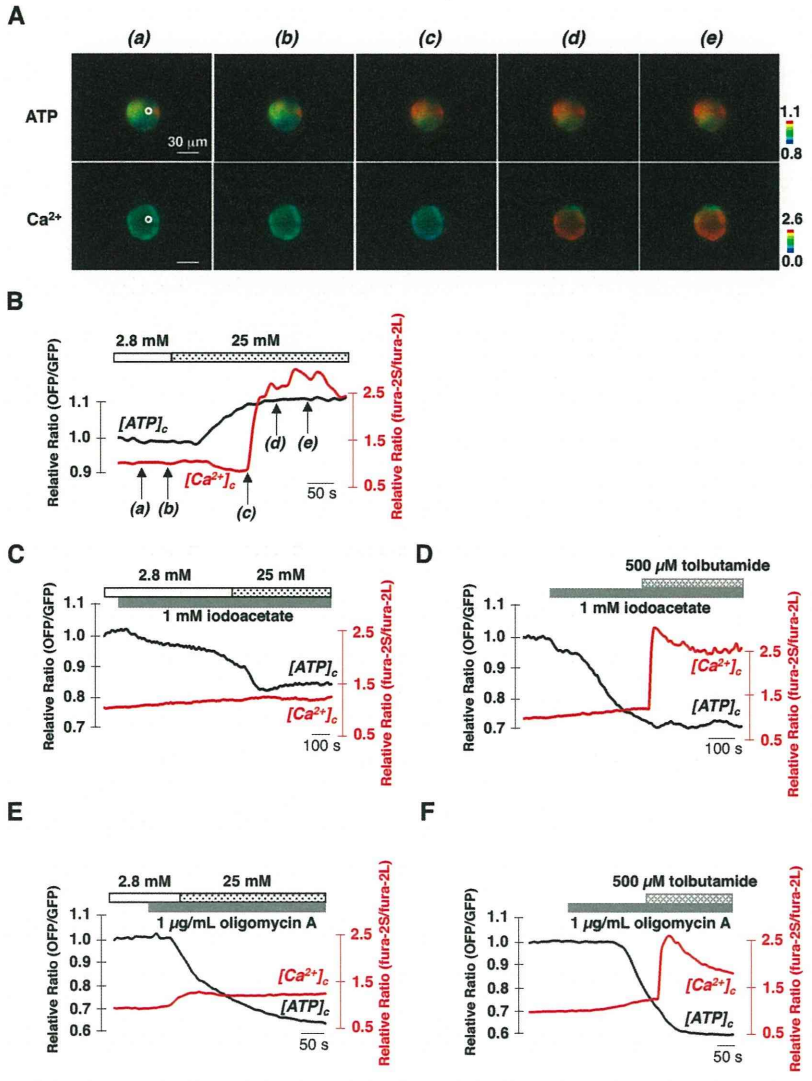
A
(a)
(b)
(c)
(d)
(e)
ATP
30 μm
1.1
0.8
Ca2+
2.6
0.0
B
2.8 mM
25 mM
Relative Ratio (OFP/GFP)
[ATP]c
[Ca2+]c
(a) (b)
(c)
(d) (e)
50 s
Relative Ratio (fura-2S/fura-2L)
C
2.8 mM
25 mM
1 mM iodoacetate
100 s
D
500 μM tolbutamide
1 mM iodoacetate
100 s
E
2.8 mM
25 mM
1 μg/mL oligomycin A
50 s
F
500 μM tolbutamide
1 μg/mL oligomycin A
50 s

Figure 6

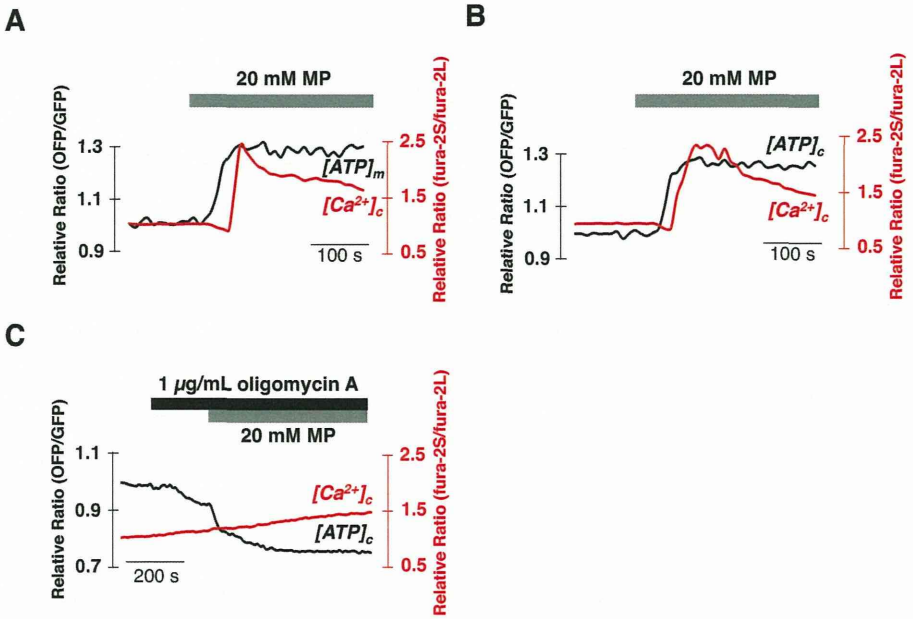
A
20 mM MP
Relative Ratio (OFP/GFP)
1.3
1.1
0.9
[ATP]m
[Ca2+]c
100 s
2.5
1.5
0.5
Relative Ratio (fura-2S/fura-2L)
B
20 mM MP
Relative Ratio (OFP/GFP)
1.3
1.1
0.9
[ATP]c
[Ca2+]c
100 s
2.5
1.5
0.5
Relative Ratio (fura-2S/fura-2L)
C
1 µg/mL oligomycin A
20 mM MP
Relative Ratio (OFP/GFP)
1.1
0.9
0.7
[Ca2+]c
[ATP]c
200 s
2.5
1.5
0.5
Relative Ratio (fura-2S/fura-2L)

Figure 7

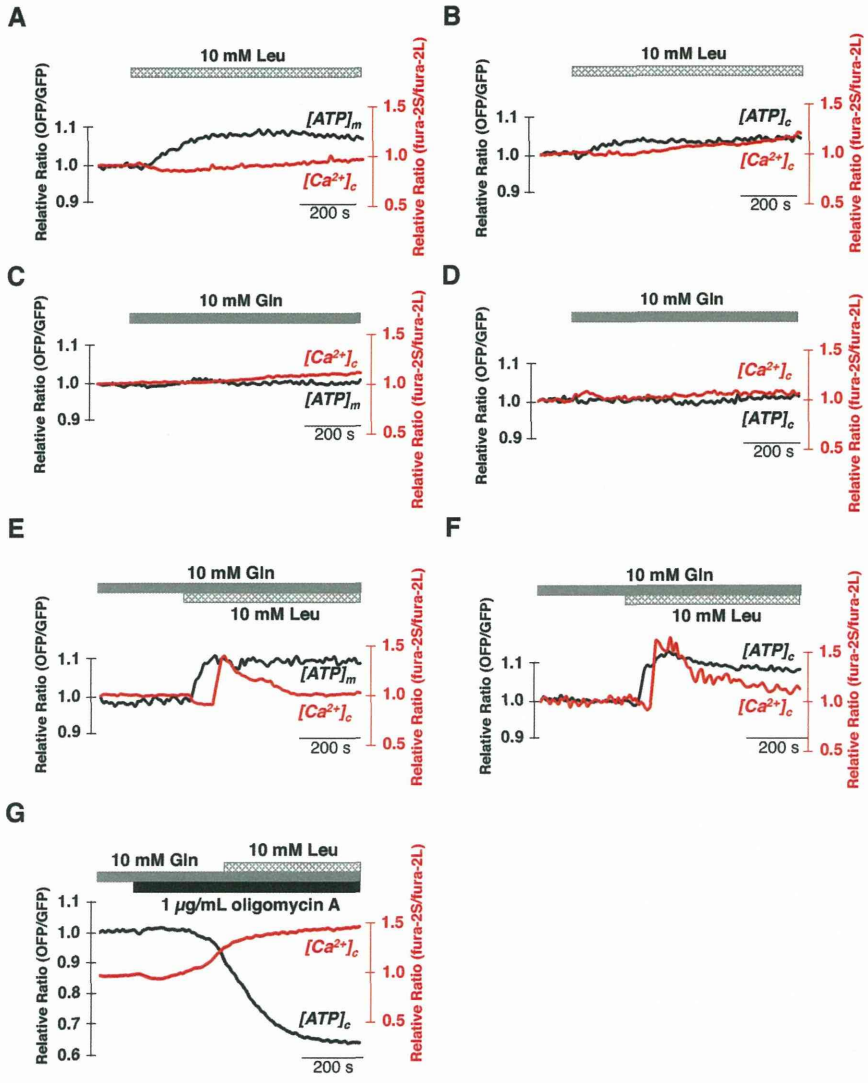
A
10 mM Leu
[ATP]m
[Ca2+]c
200 s
Relative Ratio (OFP/GFP)
Relative Ratio (fura-2S/fura-2L)
B
10 mM Leu
[ATP]c
[Ca2+]c
200 s
C
10 mM Gln
[Ca2+]c
[ATP]m
200 s
D
10 mM Gln
[Ca2+]c
[ATP]c
200 s
E
10 mM Gln
10 mM Leu
[ATP]m
[Ca2+]c
200 s
F
10 mM Gln
10 mM Leu
[ATP]c
[Ca2+]c
200 s
G
10 mM Gln
10 mM Leu
1 µg/mL oligomycin A
[Ca2+]c
[ATP]c
200 s

Figure 8

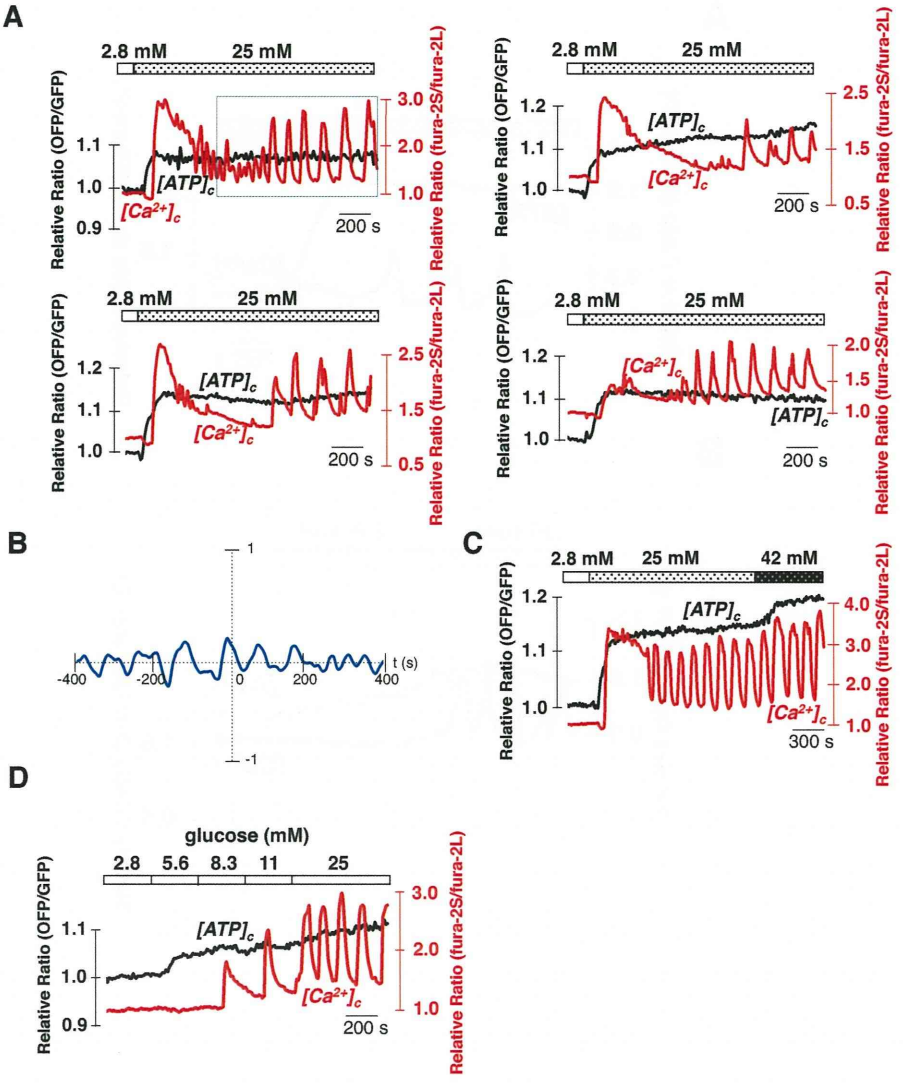
A
2.8 mM
25 mM
Relative Ratio (OFP/GFP)
Relative Ratio (fura-2S/fura-2L)
[ATP]c
[Ca2+]c
200 s
B
t (s)
-400
-200
0
200
400
1
-1
C
42 mM
300 s
D
glucose (mM)
2.8
5.6
8.3
11
25

Figure 9

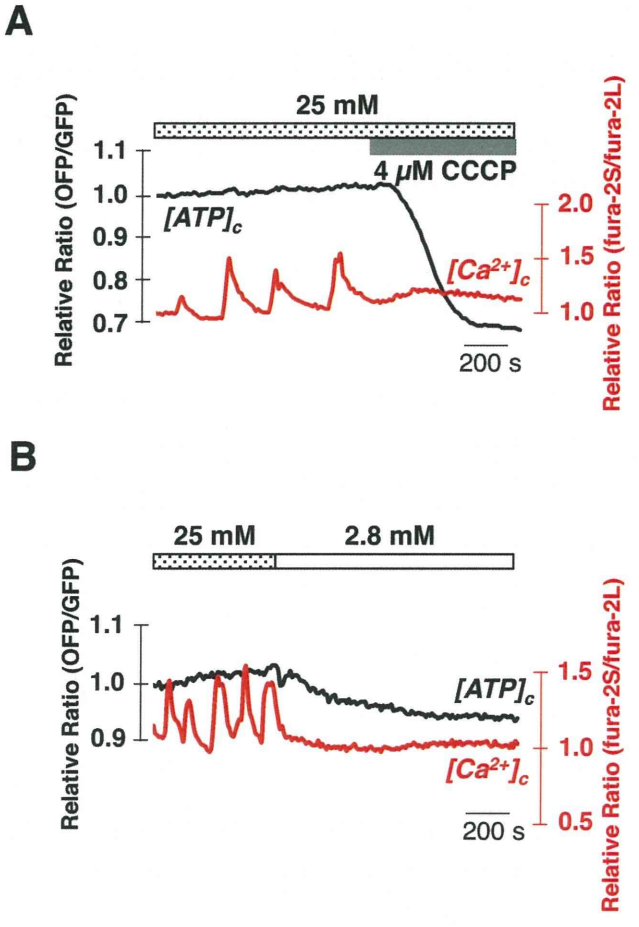
A
25 mM
4 μM CCCP
[ATP]c
[Ca2+]c
Relative Ratio (OFP/GFP)
1.1
1.0
0.9
0.8
0.7
2.0
1.5
1.0
200 s
Relative Ratio (fura-2S/fura-2L)
B
25 mM
2.8 mM
Relative Ratio (OFP/GFP)
1.1
1.0
0.9
[ATP]c
[Ca2+]c
1.5
1.0
0.5
200 s
Relative Ratio (fura-2S/fura-2L)

Figure 10

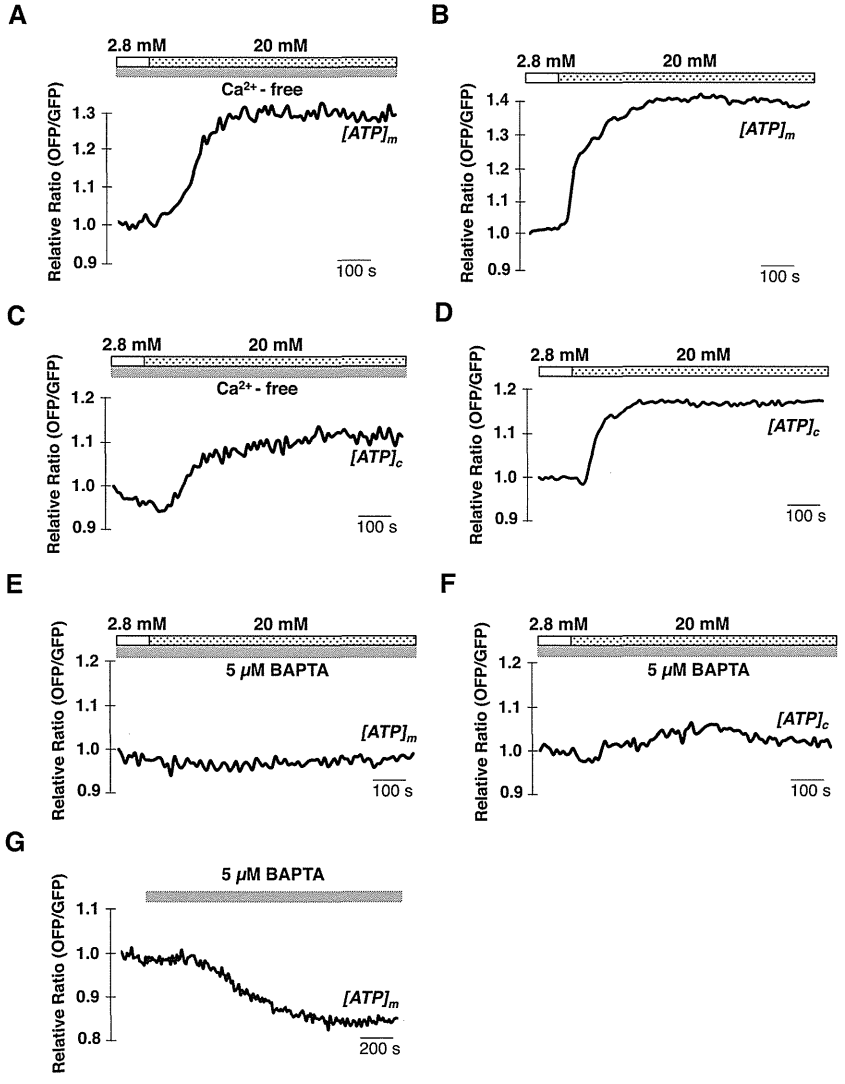
A
2.8 mM
20 mM
Ca2+ - free
[ATP]m
Relative Ratio (OFP/GFP)
1.3
1.2
1.1
1.0
0.9
100 s
B
2.8 mM
20 mM
[ATP]m
Relative Ratio (OFP/GFP)
1.4
1.3
1.2
1.1
1.0
0.9
100 s
C
2.8 mM
20 mM
Ca2+ - free
[ATP]c
Relative Ratio (OFP/GFP)
1.2
1.1
1.0
0.9
100 s
D
2.8 mM
20 mM
[ATP]c
Relative Ratio (OFP/GFP)
1.2
1.1
1.0
0.9
100 s
E
2.8 mM
20 mM
5 μM BAPTA
[ATP]m
Relative Ratio (OFP/GFP)
1.2
1.1
1.0
0.9
100 s
F
2.8 mM
20 mM
5 μM BAPTA
[ATP]c
Relative Ratio (OFP/GFP)
1.2
1.1
1.0
0.9
100 s
G
5 μM BAPTA
[ATP]m
Relative Ratio (OFP/GFP)
1.1
1.0
0.9
0.8
200 s

jbc The Journal of Biological Chemistry
AFFINITY SITES
ASBMB
American Society for Biochemistry and Molecular Biology

Metabolism:

Transcriptional Regulatory Factor X6 (Rfx6) Increases Gastric Inhibitory Polypeptide (GIP) Expression in Enteroendocrine K-cells and Is Involved in GIP Hypersecretion in High Fat Diet-induced Obesity

Kazuyo Suzuki, Norio Harada, Shunsuke Yamane, Yasuhiko Nakamura, Kazuki Sasaki, Daniela Nasteska, Erina Joo, Kimitaka Shibue, Takanari Harada, Akihiro Hamasaki, Kentaro Toyoda, Kazuaki Nagashima and Nobuya Inagaki

J. Biol. Chem. 2013, 288:1929-1938.
doi: 10.1074/jbc.M112.423137 originally published online November 28, 2012

Access the most updated version of this article at doi: 10.1074/jbc.M112.423137

Find articles, minireviews, Reflections and Classics on similar topics on the JBC Affinity Sites.

Alerts:
- When this article is cited
- When a correction for this article is posted

Click here to choose from all of JBC's e-mail alerts

This article cites 37 references, 21 of which can be accessed free at
http://www.jbc.org/content/288/3/1929.full.html#ref-list-1

Downloaded from http://www.jbc.org/ at Kyoto University on December 24, 2013

THE JOURNAL OF BIOLOGICAL CHEMISTRY VOL. 288, NO. 3, pp. 1929–1938, January 18, 2013
© 2013 by The American Society for Biochemistry and Molecular Biology, Inc. Published in the U.S.A.

Transcriptional Regulatory Factor X6 (Rfx6) Increases Gastric Inhibitory Polypeptide (GIP) Expression in Enteroendocrine K-cells and Is Involved in GIP Hypersecretion in High Fat Diet-induced Obesity*

Received for publication, September 27, 2012, and in revised form, November 28, 2012 Published, JBC Papers in Press, November 28, 2012, DOI 10.1074/jbc.M112.423137

Kazuyo Suzuki, Norio Harada, Shunsuke Yamane, Yasuhiko Nakamura, Kazuki Sasaki, Daniela Nasteska, Erina Joo, Kimitaka Shibue, Takanari Harada, Akihiro Hamasaki, Kentaro Toyoda, Kazuaki Nagashima, and Nobuya Inagaki[1]

From the Department of Diabetes and Clinical Nutrition, Graduate School of Medicine, Kyoto University, 54 Kawahara-cho, Shogoin, Sakyo-ku, Kyoto 606-8507, Japan

Background: Gastric inhibitory polypeptide (GIP) secreted from enteroendocrine K-cells potentiates insulin secretion and induces energy accumulation into adipose tissue.
Results: Transcriptional Rfx6 is expressed in K-cells and increases GIP expression. Rfx6 expression is up-regulated in K-cells of obese mice.
Conclusion: Rfx6 plays critical roles in GIP expression and hypersecretion in obesity.
Significance: Gene analysis of K-cells isolated from GIP-GFP knock-in mice enabled identification of Rfx6.

Gastric inhibitory polypeptide (GIP) is an incretin released from enteroendocrine K-cells in response to nutrient ingestion. GIP potentiates glucose-stimulated insulin secretion and induces energy accumulation into adipose tissue, resulting in obesity. Plasma GIP levels are reported to be increased in the obese state. However, the molecular mechanisms of GIP secretion and high fat diet (HFD)-induced GIP hypersecretion remain unclear, primarily due to difficulties in separating K-cells from other intestinal epithelial cells *in vivo*. In this study, GIP-GFP knock-in mice that enable us to visualize K-cells by enhanced GFP were established. Microarray analysis of isolated K-cells from these mice revealed that transcriptional regulatory factor X6 (Rfx6) is expressed exclusively in K-cells. *In vitro* experiments using the mouse intestinal cell line STC-1 showed that knockdown of Rfx6 decreased mRNA expression, cellular content, and secretion of GIP. Rfx6 bound to the region in the *gip* promoter that regulates *gip* promoter activity, and overexpression of Rfx6 increased GIP mRNA expression. HFD induced obesity and GIP hypersecretion in GIP-GFP heterozygous mice *in vivo*. Immunohistochemical and flow cytometry analysis showed no significant difference in K-cell number between control fat diet-fed (CFD) and HFD-fed mice. However, GIP content in the upper small intestine and GIP mRNA expression in K-cells were significantly increased in HFD-fed mice compared with those in CFD-fed mice. Furthermore, expression levels of Rfx6 mRNA were increased in K-cells of HFD-fed mice. These results suggest that Rfx6 increases GIP expression and content in K-cells and is involved in GIP hypersecretion in HFD-induced obesity.

Obesity leads to insulin resistance characterized by fasting hyperinsulinemia and excessive insulin secretion to maintain euglycemia after meal ingestion (1). Obesity is an important risk factor in progression to type 2 diabetes mellitus (2) as well as cardiovascular disease (3), and reduction of obesity can normalize hyperinsulinemia and impede the progression of diabetes and arteriosclerosis.

Gastric inhibitory polypeptide, also called glucose-dependent insulinotropic polypeptide (GIP),[2] and glucagon-like peptide-1 (GLP-1) are the incretins, peptide hormones released from the gastrointestinal tract into circulation in response to meal ingestion that potentiate glucose-stimulated insulin secretion (4, 5). GIP is secreted from enteroendocrine K-cells located in the duodenum and upper small intestine; GLP-1 is secreted from enteroendocrine L-cells located in the lower small intestine and colon. GIP binds to the GIP receptor (GIPR) on the surface of pancreatic β-cells, adipose tissue, and osteoblasts, and it stimulates insulin secretion (6), fat accumulation (7), and bone formation (8), respectively, by increasing the level of intracellular adenosine 3′,5′-monophosphate (cAMP).

It was reported previously that GIPR-deficient mice exhibit insufficient compensatory insulin secretion upon high fat loading (9), suggesting that GIP plays a critical role in maintaining blood glucose levels by hypersecretion of insulin in diet-induced obesity. We also reported that sensitivity of GIPR to GIP in β-cells is increased in high fat diet (HFD)-induced obese mice (10). In addition, GIPR is expressed in adipose tissue (11) and increases glucose and triglyceride uptake in fat cells (12, 13). Thus, GIP has both direct and indirect effects on the accumulation of energy into adipose tissue. Some studies report that GIP secretion is increased in obesity (7, 14–16) and that pancreatic and duodenal homeobox 1 (Pdx1), which is known to be

* This work was supported by scientific research grants from the Ministry of Education, Culture, Sports, Science, and Technology, Japan, the Ministry of Health, Labor, and Welfare, Japan, and scientific research grants from the Japan Diabetes Foundation.
[1] To whom correspondence should be addressed. Tel.: 81-75-751-3562; Fax: 81-75-751-6601; E-mail: inagaki@metab.kuhp.kyoto-u.ac.jp.

[2] The abbreviations used are: GIP, gastric inhibitory polypeptide; GIPR, GIP receptor; HFD, high fat diet; CFD, control fat diet; EGFP, enhanced GFP; OGTT, oral glucose tolerance test.

Downloaded from http://www.jbc.org/ at Kyoto University on December 24, 2013

an important transcription factor in pancreatic development and pancreatic β-cell maturation (17), has a critical role in GIP production in K-cells (18, 19). However, the mechanisms involved in GIP hypersecretion from K-cells in obesity remain unclear due to difficulties in separating these cells from other intestinal epithelial cells *in vivo*.

In this study, we investigated expression of various genes in K-cells by using GIP-GFP knock-in (GIP-GFP) mice in which K-cells can be visualized by EGFP fluorescence. We found that regulatory factor X6(Rfx6) is expressed exclusively in K-cells of the upper small intestine and is involved in GIP mRNA expression in the mouse small intestinal cell line STC-1. Furthermore, expression of Rfx6 as well as Pdx1 was found to be increased in K-cells of HFD-induced obese mice. Thus, GIP expression is stimulated by both Rfx6 and Pdx1, suggesting that these transcription factors play an important role in both GIP expression and GIP hypersecretion in HFD-induced obesity.

EXPERIMENTAL PROCEDURES

Animals—We designed targeting vector constructs as short-EGFP-poly(A)-loxp-Neo-loxp-long cassettes using mouse B6N BAC clone (identification numbers RP23-31E4 and RP23-383D10). A diphtheria toxin A expression cassette for negative selection was attached to the 3′ end of the *gip* sequence in the targeting vector. Next, the targeting vector was injected in embryonic stem cells from C57BL/6 mice, and a Neo resistance strain was established. The ES cells positive for the knock-in gene were selected by Southern blot analysis. The established ES cells were then injected into the blastocyst to obtain chimeric mice. Finally, we generated hetero-mutant mice by mating the chimeric mice with wild-type C57BL/6 mice. The mice were housed in an air-controlled (temperature 25 °C) room with a dark-light cycle of 10 and 14 h, respectively. Animal care and procedures were approved by the Animal Care Committee of Kyoto University.

GIP-GFP heterozygous mice (7 weeks of age) were fed control fat chow (CFD; 10% fat, 20% protein, and 70% carbohydrate by energy) or high fat chow (HFD; 60% fat, 20% protein, and 20% carbohydrate by energy) (Research Diets Inc., New Brunswick, NJ) for 8 weeks. Food intake, water intake, and body weight were measured.

Immunohistochemistry—Mouse upper small intestine samples were fixed in Bouin's solution and transferred into 70% ethanol before processing through paraffin. Rehydrated paraffin sections were incubated overnight at 4 °C with primary mouse anti-GFP antibody (sc-9996, 1:100, Santa Cruz Biotechnology) and rabbit anti-GIP antibody (T-4053, 1:100, Peninsula Laboratories, Inc., San Carlos, CA). Intestine samples and STC-1 cells (kindly provided by Prof. Hanahan, University of California, San Francisco) were embedded by Tissue-Tek O.C.T. compound 4583 (Sakura Fine Technical Co. Ltd., Tokyo, Japan) and immediately frozen in liquid nitrogen. Frozen sections (10 μm) on slides were air-dried and fixed in acetone for 5 min. Slides were then washed in phosphate-buffered saline (PBS) and blocked for 15 min in 3% BSA. They were incubated overnight at 4 °C with primary antibody (mouse anti-GIP antibody (1:100, kindly provided by Merck Millipore)) and goat anti-Rfx6 antibody (ABD28, 1:100, Merck). The sections were incubated for 1 h at room temperature with secondary antibody. Images were taken using a fluorescent microscopy with a BZ-8100 system (KEYENCE Corp., Osaka, Japan) and confocal microscopy with an LSM510META system (Carl Zeiss Co., Ltd., Jena, Germany).

Fifty representative mucous membranes from each slide were randomly selected, and their mean length and GFP-positive cells were quantified using fluorescent microscopy images. To count the GFP-positive cells, we distinguished the mucous membrane as villus, upper crypt, or lower crypt.

Isolation of K-cells from Mouse Intestinal Epithelium—Mouse upper small intestine was removed and washed by PBS. The intestine was cut into several round pieces and tied on one side with a thread. The pouch-like intestine was injected with Hanks' balanced salt solution containing 0.5 mg/ml collagenase, clamped, and incubated with CO_2 at 37 °C for 10 min in Krebs-Ringer bicarbonate buffer (KRBB: 120 mM NaCl, 4.7 mM KCl, 1.2 mM $MgSO_4$, 1.2 mM KH_2PO_4, 2.4 mM $CaCl_2$, 20 mM $NaHCO_3$). The digested intestinal epithelium was collected into the tube filled with Roswell Park Memorial Institute (RPMI) medium and rinsed twice. The intestinal epithelium was cultured in a humidified incubator (95% air and 5% CO_2) at 37 °C for 1 h. Afterward, it was centrifuged at 180 × *g* for 5 min, resuspended in PBS twice, and filtered with a cell strainer (352340, Falcon cell strainer, BD Biosciences). GFP-positive cells in the intestinal epithelium were analyzed using BD FACS Aria™ flow cytometer (BD Biosciences). Sorted cells were collected into vials containing medium at a rate of 2000 cells/tube.

Total RNA was extracted with PicoPure RNA isolation kit (Applied Biosystems, Inc., Alameda, CA) from sorted cells of GIP-GFP mouse intestinal epithelium and treated with DNase (Qiagen Inc., Valencia, CA). Microarray analysis was performed using GeneChip Mouse Genome 430 2.0 Array (Affymetrix Inc., Fremont, CA).

Glucose Tolerance Test (OGTT) and GIP Assay—After a 16-h fasting period, OGTTs (1 g/kg body weight) were performed. Blood samples were taken at the indicated times (0, 15, 30, 60, and 120 min after glucose loading), and blood glucose levels, plasma insulin levels, and plasma total GIP concentrations were measured. Blood glucose levels were determined by the glucose oxidase method (Sanwa Kagaku Kenkyusho Co. Ltd., Nagoya, Japan). Plasma insulin levels were determined using enzyme immunoassay (Shibayagi, Gumma, Japan). Plasma total GIP levels were determined using an ELISA kit (Merck Millipore).

For measurement of GIP content in the mouse upper small intestine, the mice were killed at 15 weeks of age after 8 weeks of CFD or HFD feeding. The intestine was rapidly removed and washed in PBS. After measuring the weight, samples were extracted with 5 ml/g acid ethanol, and GIP levels were measured (15).

Quantitative RT-PCR—Complementary DNA (cDNA) was prepared by reverse transcriptase (Invitrogen) with an oligo(dT) primer (Invitrogen). Messenger RNA (mRNA) levels were measured by quantitative RT-PCR using ABI PRISM 7000 Sequence Detection System (Applied Biosystems Inc.). PCR analyses were carried out using the oligonucleotide primers. SYBR Green PCR master mix (Applied Biosystems Inc.) was prepared for PCR run. Thermal cycling conditions were dena-

Downloaded from http://www.jbc.org/ at Kyoto University on December 24, 2013

turation at 95 °C for 10 min followed by 50 cycles at 95 °C for 15 s and 60 °C for 1 min. C- and N-terminal primers of target molecules were designed as follows: GIP forward, 5′-gtggctttgaagacctgctc-3′, and reverse, 5′-ttgttgtcggatcttgtcca-3′; GFP forward, 5′-gtggctttgaagacctgctc-3′, and reverse, 5′-tttacgtcgccgtccagctcg-3′; GLP-1 forward, 5′-tgaagacaaacgccactcac-3′, and reverse, 5′-tcatgacgtttggcaatgtt-3′; Pdx1 forward, 5′-gacctttcccgaatggaa-3, and reverse, 5′-cttgttttcctcgggttc-3′; Rfx1 forward, 5′-gcagccagaagcagtatgtg-3′, and reverse, 5′-tggcttctgacacagtctcact-3′; Rfx2 forward, 5′-cagaactccgagggaggag-3′, and reverse, 5′-ggagggtgagtgtctgcatc-3′; Rfx3 forward, 5′-cgtcacaggaggacaactca-3′, and reverse, 5′-cagacttttgcagcgtctca-3′; Rfx4 forward, 5′-ccgaatacactggccttagc-3′, and reverse, 5′-atgggtgctcctcatacagg-3′; Rfx5 forward, 5′-tctaccttcagctccatcg-3′, and reverse, 5′-ggcaggtatccatgtgctct-3′; Rfx6 forward, 5′-acagacacggaatctgacat-3′, and reverse, 5′-ctctaccacagtgtccaacc-3′; Rfx7 forward, 5′-cgctctgcaacacaagatca-3′, and reverse, 5′-gaccagaaggcagttgaagg-3′; and GAPDH forward, 5′-aaatggtgaaggtcggtgtg-3′, and reverse, 5′-tcgttgatggcaacaatctc-3′.

Cell Culture and Small Interfering RNA (siRNA) Transfection into STC-1 Cells—STC-1 cells, mouse small intestinal cell line, were cultured in Dulbecco's modified Eagle's medium (DMEM) (Sigma) supplemented with 10% heat-inactivated fetal calf serum, 100 IU/ml penicillin, and 100 μg/ml streptomycin at 37 °C in a humidified atmosphere (5% CO_2 and 95% air). siRNA transfection of Stealth™ siRNAs were synthesized (Invitrogen). The sequences of siRNAs specific for Rfx6 and Pdx1 are shown as follows: Pdx1, caguacuacgcggccacacagcucu and agagcugugguggccgcguaguacug, and Rfx6, ggugaaugccaugguaucugauauu and aauaucagauaccauggcauucacc. Cultured STC-1 cells were trypsinized, suspended with DMEM without antibiotics, mixed with Opti-MEM (Invitrogen) containing siRNA and Lipofectamine TM2000 (Invitrogen), plated on 12-well dishes, and then incubated at 37 °C in a CO_2 incubator. The amounts of STC-1 cells were 1×10^6 cells/well. Medium was replaced with 1 ml of DMEM containing antibiotics about 5–6 h after transfection. RT-PCR was performed 48 h after transfection.

Plasmid Construction and Transfection into STC-1 Cells—The cDNA fragment of mouse Rfx6 protein was obtained from mouse (C57BL/6) islets by RT-PCR. The cDNA fragment of Rfx6 was cloned into pCMV vector (Clontech). Expression plasmids of Rfx6 cDNA were transfected into STC-1 cells using Lipofectamine™ 2000 (Invitrogen). Plasmid (8 μg/well) was diluted into Opti-MEM, and Lipofectamine™ 2000 was added and incubated at room temperature for 20 min. After incubation, the mixture was added to STC-1 cells (1×10^6 cells/well). RT-PCR was performed 48 h after transfection.

Measurement of Incretin Release and Cellular Content in STC-1 Cells—For incretin release assays, DMEM was collected from STC-1 cells cultured on 12-well dishes about 42–43 h after changing the medium (48 h after transfection). Media were centrifuged at $3000 \times g$ for 10 min, and the supernatant was collected. Total GIP and total GLP-1 levels were measured by ELISA methods (Merck Millipore and Meso Scale Discovery (Gaithersburg, MD), respectively) as incretin release from STC-1 cells.

To determine incretin content, STC-1 cells cultured on 12-well dishes (48 h after transfection) were washed with PBS and homogenized in 0.5 ml of 0.1 N HCl and extracted at RT for 10 min, after which the supernatant was collected and centrifuged at $3000 \times g$ for 10 min. Incretin and protein levels were measured by ELISA (GIP and GLP-1) and Bradford reagent (Bio-Rad), respectively.

Yeast One-hybrid Assay—Yeast one-hybrid assays were performed using the Matchmaker Gold Yeast One-hybrid Library Screening System (Clontech) according to the manufacturer's protocol. The *gip* promoter fragments shown in Fig. 4*A* were inserted separately upstream of the aureobasidin A resistance gene on the pAbAi vector, and Rfx6 cDNA was inserted downstream of GAL4-activating domain (GAL4AD) on the pGADT7 activating domain vector. The interactions between *gip* promoter fragments and Rfx6-GAL4AD protein were assayed using the aureobasidin A resistance gene reporter system. First, *Saccharomyces cerevisiae* Y1HGold (*MATα, ura3-52, his3-200, ade2-101, trp1-901, leu2-3, 112, gal4Δ, gal80Δ, met-MEL1*) was transformed by *gip* promoter fragment-inserted pAbAi plasmid (pAbAi-fragments a, b, c, and d), and spread on the synthetic medium with dextrose (SD) (without uracil) and incubated for 1 week at 30 °C. Obtained yeast was transformed by Rfx6 cDNA-inserted pGADT7 activating domain plasmid (pGADT7-Rfx6), spread on the SD (without tryptophan) medium, and then incubated for 1 week at 30 °C. Interaction between *gip* promoter fragment and Rfx6-GAL4AD protein could be detected, and the transformant was grown on SD (without tryptophan) medium containing 600 ng/ml aureobasidin A.

GIP Promoter Activity—1×10^6 STC-1 cells were cotransfected with pGL4.19 luciferase reporter plasmid expressing five different lengths of the *gip* promoter gene (Fig. 4*C*) and pGL4.73 *Renilla* luciferase reporter plasmid. 48 h after transfection, luciferase and *Renilla* activities were assayed according to the manufacturer's protocol (Promega Corp., Madison, WI) using a GioMax 20/20n luminometer (Promega). Firefly luciferase activity was normalized to *Renilla* luciferase expression and is presented as fold increase in relative light units over samples transfected with pGL4.19. All samples were analyzed in duplicate.

Analysis—The results are given as means ± S.E. (S.E., n = number of mice). Statistical significance was determined using paired and unpaired Student's t test and analysis of variance. $p \leq 0.05$ was considered significant.

RESULTS

Visualization and Isolation of K-cells Using GIP-GFP Mice—GIP-GFP mice were generated for the purpose of visualizing enteroendocrine K-cells (Fig. 1*A*). The mouse *gip* gene is composed of six exons. The targeting vector for GIP-GFP mice was designed so that EGFP cDNA was fused with exon 3 in the *gip* gene. Prepro-GIP consists of 144 amino acids (Fig. 1*B*), and PC1/3 and PC2 cleave prepro-GIP, generating GIP(1–42) and GIP(1–30), respectively. In GIP-GFP mice, the fusion protein retains the signal peptide, but it does not have the GIP(1–42) sequence nor the PC1/3 and PC2 cleavage sites. Accordingly, GIP-GFP mice express GIP signal peptide-GFP fusion protein

Downloaded from http://www.jbc.org/ at Kyoto University on December 24, 2013

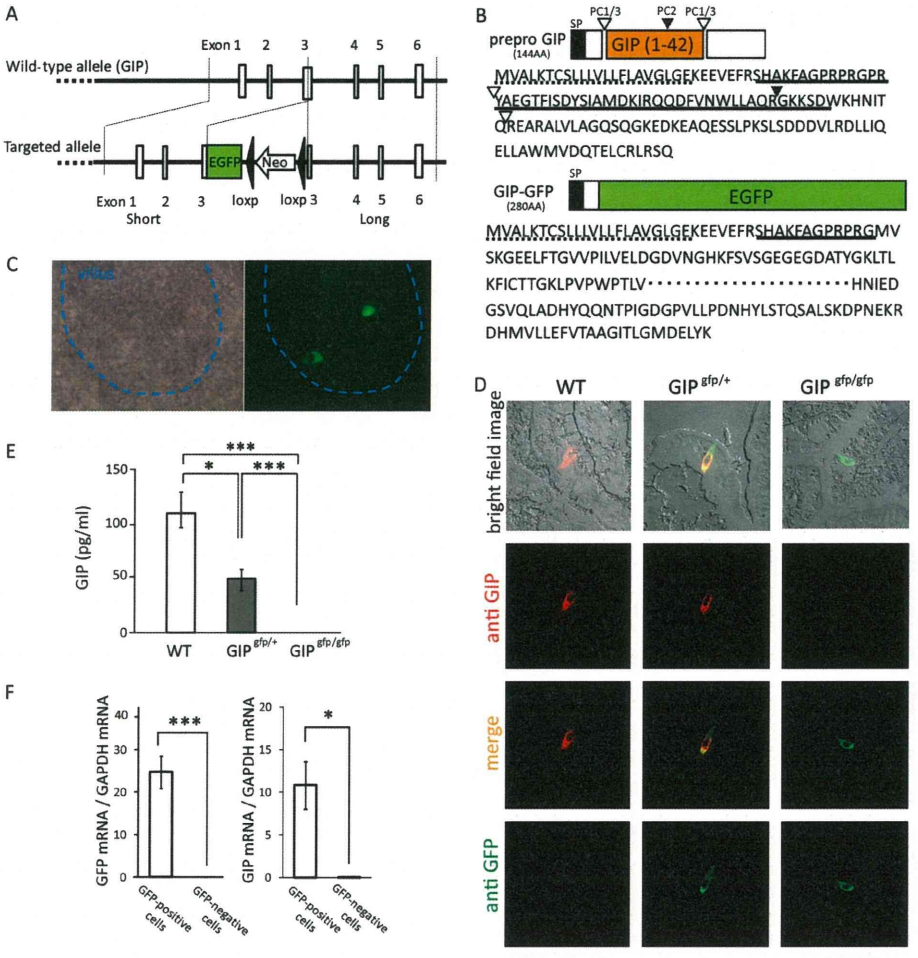

FIGURE 1. **Gene construct of GIP-GFP mice.** *A,* wild-type GIP allele and targeted allele of GIP-GFP. EGFP-poly(A)-loxp-Neo-loxp cassette was inserted into exon 3 of wild-type *gip* gene. *B,* prepro-GIP protein and GIP-GFP fusion protein. *SP,* signal peptide. *Open triangle,* PC1/3 cleavage site; *closed triangle,* PC2 cleavage site; *dotted line,* amino acids of signal peptide; *solid line,* translated protein from exon 3. *C,* microscopic images of upper small intestine in GIP-GFP heterozygous mice (bright field image and fluorescence image). *D,* immunohistochemical images of upper small intestine in wild-type (*WT*), GIP-GFP heterozygous ($GIP^{gfp/+}$), and homozygous mice ($GIP^{gfp/gfp}$). *Green,* GFP-expressing cells; *red,* GIP-expressing cells; *yellow,* merged image. *E,* fasting plasma GIP levels in WT, $GIP^{gfp/+}$, and $GIP^{gfp/gfp}$ mice. *F,* GFP mRNA and GIP mRNA levels in GFP-positive cells ($n = 5–6$) and GFP-negative cells ($n = 5–6$). *, $p \leq 0.05$; **, $p \leq 0.01$; ***, $p \leq 0.001$.

(280 amino acids). GFP fluorescence was observed in the small intestine of GIP-GFP heterozygous mice (Fig. 1*C*) and GIP-GFP homozygous mice (data not shown).

Immunohistochemical analysis was performed to assess localization of GFP-expressing cells and GIP-expressing cells using anti-GFP and anti-GIP antibodies, respectively, in the upper small intestine of wild-type and GIP-GFP heterozygous and homozygous mice (Fig. 1*D*). GFP-expressing cells are present in the intestine of GIP-GFP heterozygous and homozygous mice and GIP-expressing cells are present in the intestine of both wild-type and GIP-GFP heterozygous mice. However, in GIP-GFP homozygous mice, no GIP-expressing cells were found. The GFP-expressing cells were identical to the GIP-expressing cells in the GIP-GFP heterozygous mice. We then examined the fasting plasma GIP levels in the three types of mice (Fig. 1*E*). GIP levels were significantly lower in GFP-GFP heterozygous mice compared with those in wild-type mice. GIP levels of GIP-GFP homozygous mice were not detectable. These results indicate that GIP-GFP heterozygous mice have only one normal *gip* gene and that GIP-GFP homozygous mice have no normal *gip* genes.

Next, GFP-positive cells were purified by a flow cytometry system. GFP-positive cells and GFP-negative cells from upper small intestinal epithelium of GIP-GFP heterozygous mice were separated and collected. GFP mRNA and GIP mRNA were highly expressed in GFP-positive cells (Fig. 1*F*). In microarray analysis, the expression levels of GIP mRNA were much higher in GFP-positive cells than those in GFP-negative cells (GFP-positive cells ($n = 3$) 12,951.55 ± 335.77 *versus* GFP-negative cells ($n = 3$) 1763.61 ±142.65; $p \leq 0.001$). These results demonstrate that the GFP-positive cells in the intestinal epithelium of GIP-GFP mice are K-cells.

Transcription Factor Rfx6 Is Expressed Exclusively in K-cells—Microarray analysis data revealed that mRNA of the transcription factor Rfx6 is highly expressed in GFP-positive cells (GFP-positive cells ($n = 3$) 2613.4 ± 341.9 *versus* GFP-negative cells ($n = 3$) 24.0 ± 6.7; $p \leq 0.05$). As seven members of the Rfx family were identified previously, we evaluated the expression

Downloaded from http://www.jbc.org/ at Kyoto University on December 24, 2013

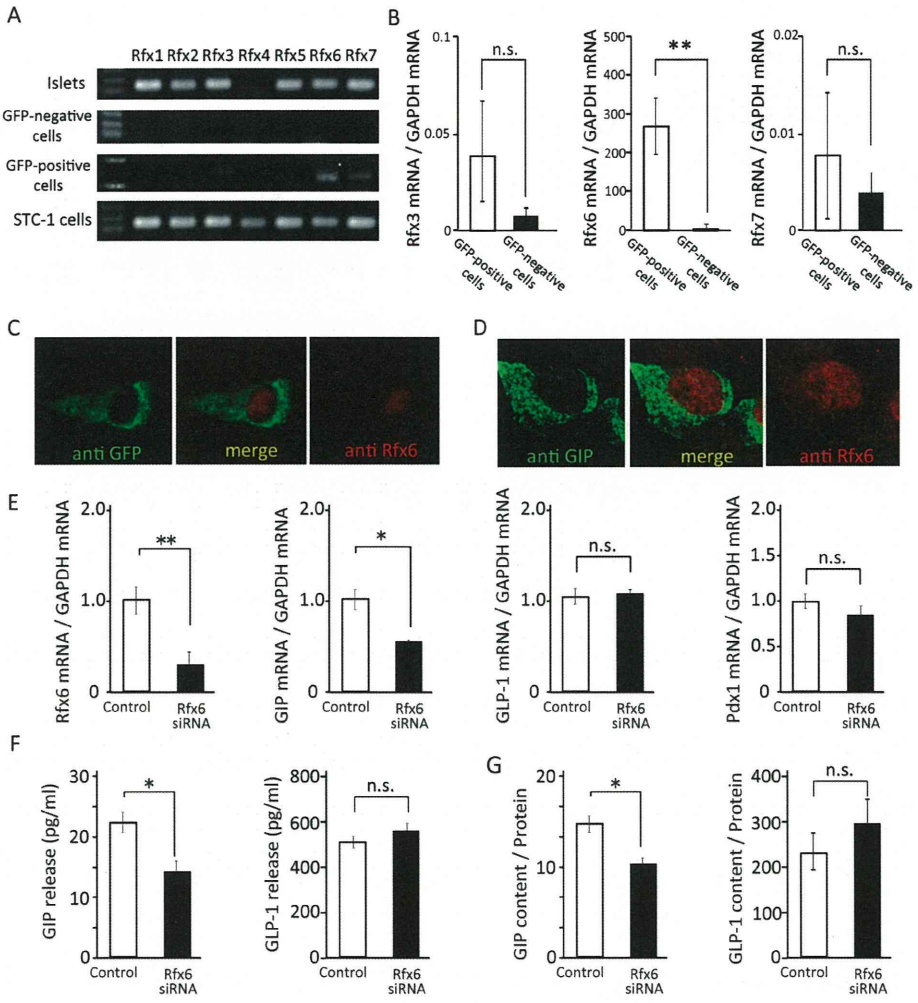

FIGURE 2. **Effect of Rfx6 on mRNA expression, cellular content, and secretion of GIP in STC-1 cells.** *A,* mRNA expression for *rfx* genes 1–7 in islets, GFP-negative cells, GFP-positive cells, and STC-1 cells by PCR. *B,* Rfx3, Rfx6, and Rfx7 mRNA levels in GFP-positive cells (n = 8–10) and GFP-negative cells (n = 8–10). *C,* immunohistochemical images of upper small intestine in GIP-GFP heterozygous mice. *Green,* GFP-expressing cells; *red,* Rfx6-expressing cells; *yellow,* merged image. *D,* immunohistochemical images of STC-1 cells. *Green,* GIP-expressing cells; *red,* Rfx6-expressing cells; *yellow,* merged image. *E,* Rfx6, GIP, GLP-1, and Pdx1 mRNA levels in Rfx6 knockdown STC-1 cells (n = 4). *F* and *G,* incretin content and secretion in Rfx6 knockdown STC-1 cells (n = 4). *, $p \leq 0.05$; **, $p \leq 0.01$, *n.s.*, not significant.

of these mRNAs in mouse islets, GFP-positive cells (K-cells), and mouse small intestinal cell line STC-1 (Fig. 2*A*). All of the *rfx* genes, except for *rfx4*, were expressed in islets as shown in a previous study (20). Rfx3, Rfx6, and Rfx7 were expressed in GFP-positive cells, but no Rfx mRNAs were detected in the GFP-negative cells. In semi-quantitative RT-PCR data, the expression levels of Rfx6 were extremely higher in GFP-positive cells than those in GFP-negative cells, whereas the expression levels of Rfx3 and Rfx7 were similar (Fig. 2*B*). Immunohistochemistry confirmed that Rfx6-expressing cells correspond to GFP-expressing cells (Fig. 2*C*), demonstrating that Rfx6 is expressed exclusively in K-cells.

Inhibition of Rfx6 and Pdx1 Expression Decreases GIP Expression in STC-1 Cells—We then assessed the influence of Rfx6 on GIP expression and secretion by using STC-1 cells. Rfx6 mRNA expression was confirmed in STC-1 cells by RT-PCR (Fig. 2*A*). The Rfx6-expressing cells were similarly located in the GIP-expressing cells by immunohistochemistry (Fig. 2*D*). By treatment with Rfx6 siRNA, Rfx6 mRNA expression was inhibited by 70% (Fig. 2*E*). In the same condition, mRNA expression, cellular content, and secretion of GIP were significantly decreased whereas those of GLP-1 were similar to control (Fig. 2, *E–G*), indicating that Rfx6 increases GIP mRNA expression, cellular content, and secretion. However, Pdx1 is reported to be an important transcriptional factor for producing GIP in K-cells (17, 18), although its expression levels were similar in GFP-positive and GFP-negative cells (Fig. 3*A*). To examine the effect of Pdx1 on incretin expression and secretion, mRNA expression, cellular content, and secretion of GIP and GLP-1 were measured in Pdx1-knockdown STC-1 cells by using siRNA. Pdx1 mRNA expression was confirmed in STC-1 cells by RT-PCR (Fig. 3*B*). The expression levels of Pdx1 mRNA were decreased by 50% in STC-1 cells treated with Pdx1 siRNA (Fig. 3*C*). GIP mRNA expression, cellular content, and secretion were significantly decreased, whereas GLP-1 mRNA expression, cellular content, and secretion were somewhat increased in STC-1 cells treated with Pdx1 siRNA (Fig. 3, *C–E*). The expression levels of Rfx6 mRNA were significantly decreased in the cells (Fig. 3*C*).

Downloaded from http://www.jbc.org/ at Kyoto University on December 24, 2013

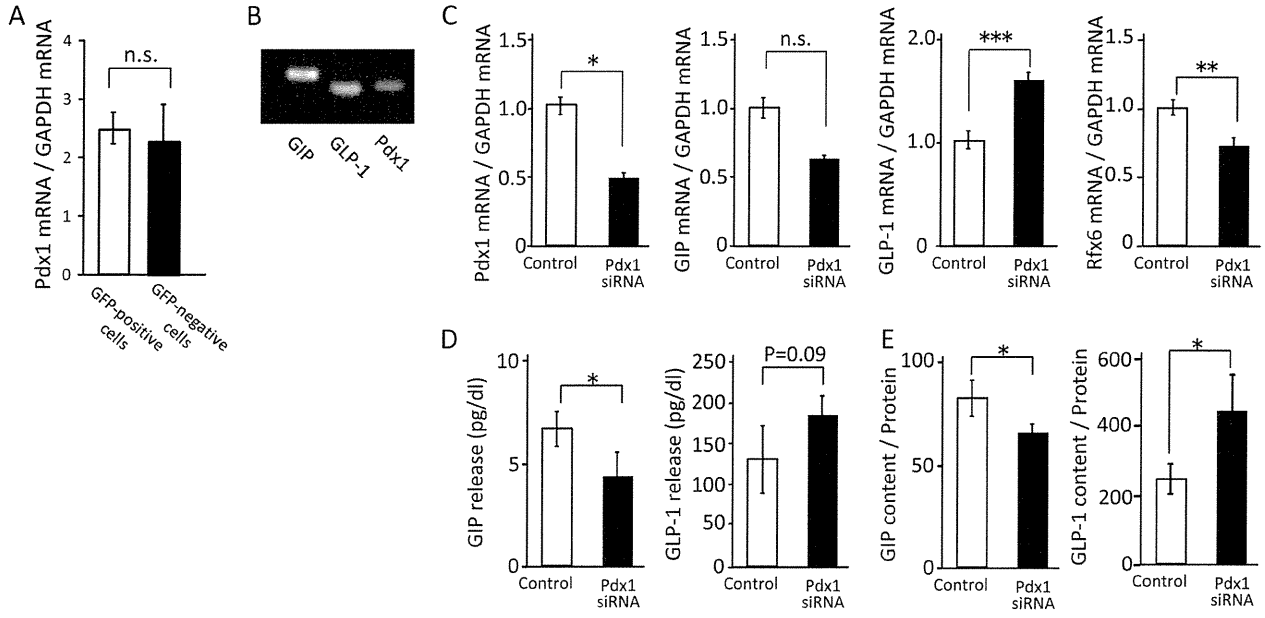

FIGURE 3. **Effect of Pdx1 on mRNA expression, cellular content, and secretion of GIP.** *A*, Pdx1 mRNA levels in GFP-positive cells and GFP-negative cells (n = 8–10). *B*, GIP, GLP-1, and Pdx1 mRNA expressions in STC-1 cells by RT-PCR. *C*, Pdx1, GIP, GLP-1, and Rfx6 mRNA levels in Pdx1 knockdown STC-1 cells (n = 4). *D* and *E*, incretin content and secretion in Pdx1 knockdown STC-1 cells (n = 4). *, $p \leq 0.05$; **, $p \leq 0.01$; ***, $p < 0.001$, *n.s.*, not significant.

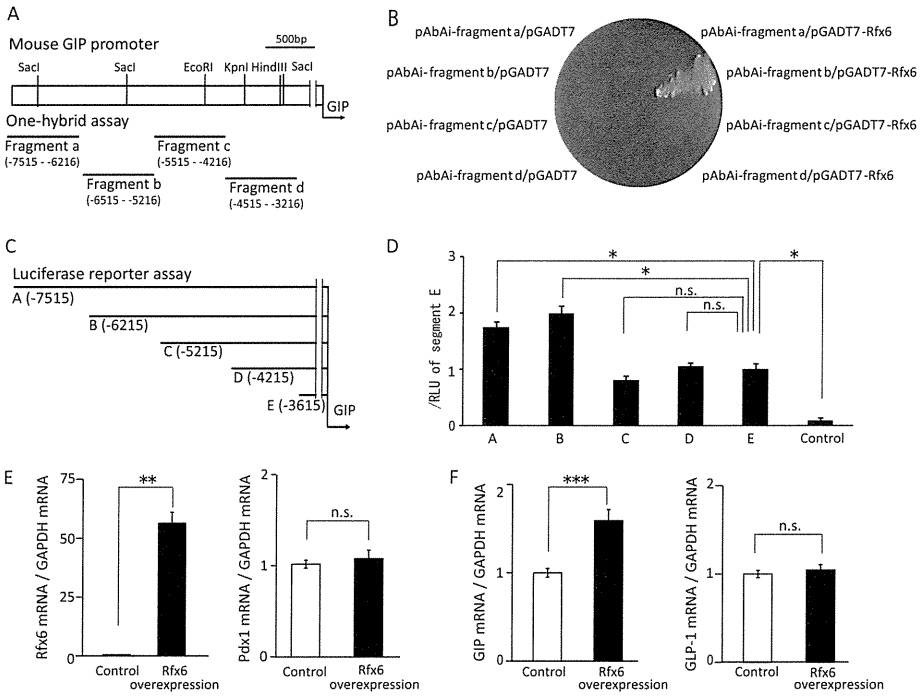

FIGURE 4. **Interaction of Rfx6 and *gip* gene.** *A*, design of the *gip* promoter fragments for one-hybrid assay. *Numbers* indicate nucleotides upstream from the transcription start site of the *gip* gene. *B*, results of yeast one-hybrid assay. Only yeast transformed with both pAbAi vector containing fragment b (*pAbAi-fragment b*) and Rfx6 cDNA-inserted pGADT7 (*pGADT7-Rfx6*) was grown on SD medium. *C*, design of the different lengths of *gip* promoter genes for luciferase reporter plasmid transfected in STC-1 cells. *D*, luciferase promoter assay on *gip* promoter. Data are represented by ratio of relative light units (*RLU*) of fragment E (n = 3–4). *, $p \leq 0.05$, *n.s.*, not significant. *E* and *F*, Pdx1, Rfx6, GIP, and GLP-1 mRNA levels in Rfx6-overexpressing STC-1 cells. **, $p \leq 0.01$; ***, $p \leq 0.001$ *versus* control, *n.s.*, not significant.

Interaction of Rfx6 and GIP Gene—We assessed the interaction of the Rfx6 and *gip* gene by one-hybrid assay. Four fragments of the *gip* promoter were constructed (Fig. 4*A*). Rfx6 effectively bound to fragment b (5216–6512 base pairs (bp) upstream of the *gip* promoter) (Fig. 4*B*). In the luciferase promoter assay, *gip* promoter activity of fragments A and B containing 5216–6512 bp upstream of *gip* promoter was high, whereas the activities of *gip* promoter C, D, and E were significantly decreased (Fig. 4*D*). These results suggest that Rfx6 binds to the region 5216–6512 bp upstream of the *gip* promoter,

Downloaded from http://www.jbc.org/ at Kyoto University on December 24, 2013

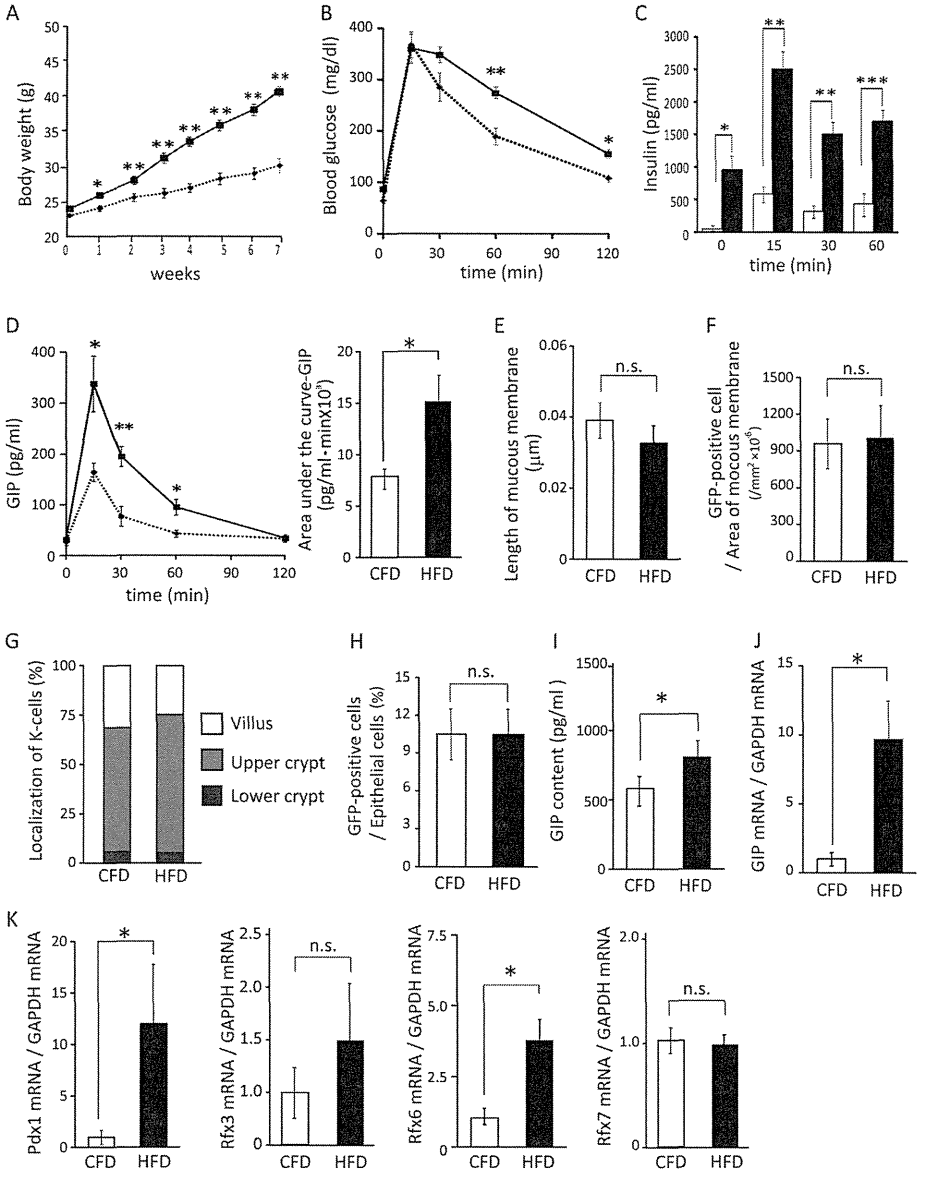

FIGURE 5. **Analysis of K-cells in the small intestine of CFD- and HFD-fed GIP-GFP heterozygous mice (histology, flow cytometry analysis, and gene expression).** *A*, body weight change of CFD-fed (*dashed line*) and HFD-fed (*continuous line*) GIP-GFP heterozygous mice (n = 5–7). *B–D*, blood glucose (*B*), insulin (*C*), and GIP levels (*D*) during OGTT after 8 weeks of CFD- or HFD-feeding (n = 5). *Dashed line* and *white box* shows CFD group, and *continuous line* and *black box* shows CFD group. *, $p \leq 0.05$; **, $p \leq 0.01$; ***, $p \leq 0.001$ *versus* CFD-fed mice. *E*, length of mucous membrane in upper small intestine (n = 5). *F*, number of GFP-positive cells by immunohistochemistry (n = 5). *G*, localization of K-cells in the upper small intestine by immunohistochemistry (n = 5). *H*, number of K-cells in the upper small intestine by flow cytometry analysis (n = 5). *I*, GIP content in upper small intestine (n = 5–7). *J*, GIP mRNA levels in GFP-positive cells (n = 8–10). *K*, Pdx1, Rfx3, Rfx6, and Rfx7 mRNA levels in GFP-positive cells (n = 8–10). *, $p \leq 0.05$; *n.s.*, not significant.

which regulates the *gip* promoter activity. Furthermore, Rfx6 was overexpressed in STC-1 cells by transfection of Rfx6 expression plasmids. The expression levels of Rfx6 mRNA levels were significantly higher in Rfx6-overexpressing cells compared with control (Fig. 4*E*). Rfx6 had no effect on the expression levels of to Pdx1 mRNA. GIP mRNA expression levels were significantly increased in Rfx6-overexpressing cells, but GLP-1 mRNA expression levels were not (Fig. 4*F*).

HFD Feeding Increases GIP Secretion and Induces Obesity and Insulin Hypersecretion in GIP-GFP Heterozygous Mice—To investigate the mechanisms of GIP hypersecretion in HFD-induced obesity *in vivo*, GIP-GFP heterozygous mice were fed CFD or HFD for 8 weeks. One week after starting these diets, the body weight of the HFD group was significantly increased compared with that of the CFD group (Fig. 5*A*). There was no difference in food and water intake between the CFD and HFD groups (data not shown). After CHD or HFD feeding for 8 weeks, OGTTs were performed. Blood glucose levels were significantly increased at 60 and 120 min during OGTT in HFD group (Fig. 5*B*). Insulin levels also were significantly increased in the HFD group (Fig. 5*C*). Insulin secretion (area under the curve-insulin) of the HFD group was increased about 5.5-fold compared with that of the CFD group (CFD group (n = 6) 38,221 ± 238 *versus* HFD group (n = 6) 211,835 ± 456; $p \leq$

Downloaded from http://www.jbc.org/ at Kyoto University on December 24, 2013

0.001). GIP concentrations of HFD group at 15, 30, and 60 min were increased significantly compared with those of the CFD group (Fig. 5*D*). GIP secretion (area under the curve-GIP) of the HFD group was increased about 1.5-fold compared with that of the CFD group (CFD group ($n = 6$) 7368 ± 123 *versus* HFD group ($n = 6$) 10,531 ± 216; $p \leq 0.05$) These results show that HFD feeding increases GIP secretion and induces obesity and insulin hypersecretion in GIP-GFP heterozygous mice, which have only one normal *gip* gene.

GIP Hypersecretion in HFD-induced Obese Mice Is Not Due to Increase of K-cell Number but to Increase of GIP Expression in K-cells—To determine whether GIP hypersecretion involves an increased number of K-cells in HFD-fed GIP-GFP heterozygous mice, the number and localization of the K-cells in the upper small intestine were estimated and compared. The length of the mucous membrane and the number and localization of K-cells examined by immunohistochemistry were similar in the CFD and HFD group (Fig. 5, *E–G*). Flow cytometry analysis also showed no difference in K-cell number between the two groups (Fig. 5*H*). However, GIP content in the upper small intestine was significantly increased in the HFD group compared with that in the CFD group (Fig. 5*I*). In addition, in K-cells purified using flow cytometry, the expression levels of GIP mRNA were almost 10-fold higher in the HFD group than those in the CFD group (Fig. 5*J*). These results demonstrate that GIP hypersecretion under HFD-induced obesity is not due to an increase in K-cell number but to an increase of GIP mRNA expression and content in K-cells.

Rfx6 and Pdx1 mRNA Levels Were Increased in K-cells of HFD-induced Obese Mice—We also assessed the expression of other candidate genes in K-cells (GFP-positive cells) (Fig. 5*K*) and non-K-cells (GFP-negative cells). Both Rfx6 and Pdx1 mRNA levels were increased in K-cells of the HFD group compared with those in K-cells of the CFD group, but the mRNA expression levels of Rfx3 and Rfx7 were not. Other Rfx transcriptional factors (Rfx1, -2, -4, and -5) were not detected in the K-cells of HFD-fed mice. Furthermore, none of the Rfx transcriptional factors were detected in non-K-cells. Pdx1 mRNA expression was detected in non-K-cells, but there was no significant difference in the expression level between the CHD group and the HFD group (ratio of Pdx1 mRNA to GAPDH mRNA: CFD group ($n = 8$) 0.47 ± 0.15 *versus* HFD group ($n = 8$) 0.26 ± 0.08; $p = 0.24$). These results strongly suggest that an increase in Rfx6 expression as well as Pdx1 expression in K-cells stimulates GIP mRNA expression and content in K-cells of HFD-fed obese mice.

DISCUSSION

Analysis of K-cells *in vivo* has been impossible due to the inability to isolate the GIP-producing K-cells from intestinal epithelium. In this study, GIP-GFP mice enabled sorting GFP-positive cells as K-cells and revealed that the transcription factor Rfx6 is expressed exclusively in K-cells by microarray analysis and RT-PCR (Fig. 2*B*). Rfx3 and Rfx7 also were detected in K-cells by RT-PCR, but there were no significant differences in their expression between K-cells and non-K-cells (Fig. 2*B*). The *rfx* gene family of transcription factors was first detected in mammals as regulatory factors that bind to the promoter regions of major histocompatibility complex (*MHC*) class II genes (21); seven types of Rfx (Rfx1–7) have so far been identified. All Rfx transcription factors have a winged helix DNA binding domain. Rfx1–4 and -6 have a dimerization domain (22, 23), and Rfx6 forms homodimers or heterodimers with Rfx2 or Rfx3 (24, 25). Rfx6 was initially isolated from human genome sequences in 2008 (22). Serial Analysis of Gene Expression (SAGE) frequency data showed high expression of Rfx6 mRNA in the pancreas, liver, and heart, and RT-PCR analysis showed high expression of Rfx6 mRNA in human pancreas and intestine (20). However, it is known that Rfx3 mRNA is expressed in brain, placenta, pancreas, and pituitary and that Rfx3 directly regulates the promoters of *glut2* and glucokinase in pancreatic β-cells (26). Rfx7 is known to be expressed in many different tissues. *rfx3*- and *rfx6*-deficient mice were generated previously, and none of the endocrine cells, excluding pancreatic polypeptide-expressing cells, are detected in the islets of these mice (20, 27). These results suggest that Rfx3 and Rfx6 play a critical role in generating the endocrine cells in islets, but it is unknown whether they are associated with generation of enteroendocrine cells such as K-cells and L-cells. We examined incretin mRNA expression and content under the inhibition of Rfx6 expression in STC-1 cells. Other incretin GLP-1 mRNA expression and content were preserved in Rfx6-knockdown STC-1 cells. However, GIP mRNA expression and content were significantly decreased in the cells (Fig. 2, *E–G*). In addition, Rfx3 expression tended to be higher in GFP-positive cells than that in GFP-negative cells (Fig. 2*B*), but GIP mRNA expression, content, and secretion were not changed in Rfx3-knockdown STC-1 cells (data not shown). These results suggest that Rfx6 expressed exclusively in K-cells plays an important role in GIP expression, cellular content, and secretion in K-cells. In addition, we examined the effect of Rfx6 on the *gip* gene and found that Rfx6 binds to the region 5216–6512 bp upstream of the *gip* promoter gene (Fig. 4*D*) and that Rfx6 increased GIP mRNA expression in STC-1 cells (Fig. 4*F*). Further study is needed to clarify the regulatory mechanism of *gip* promoter activity by Rfx6. In previous studies, characterization of K-cells and microarray analysis were done using purified K-cells from the intestine of transgenic mice expressing a yellow fluorescent protein (YFP) under the control of the 200-kb rat *gip* promoter (28, 29), but Rfx6 expression in K-cells was not reported. The reason such a long promoter is required for specific expression of YFP in K-cells is not known, but it suggests that regulation of *gip* gene expression is under complex control. In this study, we established GIP-GFP mice in which GFP is under an endogenous native promoter. Using these GIP-GFP mice, we were able to determine that Rfx6 is expressed exclusively in K-cells.

In previous studies, Pdx1 expression was detected in K-cells, and *pdx1*-deficient mice showed a greatly decreased number of GIP-expressing cells in the intestine (18, 19). It also has been reported that Pdx1 binds 150 bp upstream of the *gip* promoter, activates the *gip* promoter in STC-1 cells, and that Pdx1 expression is essential for producing GIP in K-cells (18, 19). We found that there was no significant difference in Pdx1 mRNA expression between upper small intestinal K-cells and non-K-cells (Fig. 3*A*). These findings suggest the possibility that Rfx6 spe-

Downloaded from http://www.jbc.org/ at Kyoto University on December 24, 2013